Excited Doublet States of Electrochemically Generated Aromatic Imide and Diimide Radical Anions

David Gosztola,* Mark P. Niemczyk, and Walter Svec

Chemistry Division, Argonne National Laboratory, Argonne, Illinois 60439-4831

Aaron S. Lukas and Michael R. Wasielewski*,†

Department of Chemistry, Northwestern University, Evanston, Illinois 60208-3113

Received: February 22, 2000; In Final Form: May 17, 2000

The radical anions of aromatic diimides have been implicated recently in a wide variety of photochemical electron transfer reactions. Photoexcitation of these radical anions produces powerfully reducing species. Yet, the properties of the π^* excited doublet states of these organic radical anions remain obscure. The radical anions of three aromatic imides with increasingly larger π systems, *N*-(2,5-di-*tert*-butylphenyl)phthalimide, **1**, *N*-(2,5-di-*tert*-butylphenyl)-1,8-naphthalimide, **2**, and *N*-(2,5-di-*tert*-butylphenyl)perylene-3,4-dicarboximide, **3**, as well as the three corresponding aromatic diimides, *N*,*N*′-bis(2,5-di-*tert*-butylphenyl)pyromellitimide, **4a**, *N*,*N*′-bis(2,5-di-*tert*-butylphenyl)-naphthalene-1,8:4,5-tetracarboxydiimide, **5a**, and *N*,*N*′-bis(2,5-di-*tert*-butylphenyl)perylene-3,4:9,10-tetracarboxydiimide, **6**, were produced by electrochemical reduction of the neutral molecules in an optically transparent thin layer electrochemical cell. The radical anions of these imides and diimides all exhibit intense visible and weaker near-IR absorption bands corresponding to their $D_0 \rightarrow D_n$ transitions. Excited states of the radical anions were generated by subpicosecond excitation into these absorption bands. Excitation of $\mathbf{1}^{\bullet-}$ and $\mathbf{2}^{\bullet-}$ resulted in decomposition of these radical anions, whereas excitation of $\mathbf{3}^{\bullet-}-\mathbf{6}^{\bullet-}$ yielded transient spectra of their $D_1 \rightarrow D_n$ transitions and the lifetimes of D_1. The lifetimes of the D_1 excited states of the radical anions of $\mathbf{3}^{\bullet-}-\mathbf{6}^{\bullet-}$ are all less than 600 ps and increase as the D_0-D_1 energy gap increases. These results impose design constraints on the use of these excited radical anions as electron donors in electron-transfer systems targeted toward molecular electronics and solar energy conversion.

Introduction

Photoexcited radical ions have been shown to be powerful redox agents in mechanistic and electron-transfer studies.[1−8] Spectroscopic techniques such as fluorescence and transient absorption have been used to directly probe the photophysical properties of radical ion excited states and have shown that these properties are very different from those of the neutral parent molecule.[7−19] In some cases it has been found that the excited states of radical ions of highly fluorescent molecules are themselves either weakly fluorescent or nonfluorescent.[4,14,20] This property has recently been exploited to implement an optical molecular switch concept.[21] Many studies of radical ion excited states have involved quinone or quinone-like molecules in which the radical anion is produced either electrochemically or pulse radiolytically. One of the reasons quinone radical anions have received so much attention is their role as electron acceptors in numerous donor−acceptor molecules designed to mimic photosynthetic charge separation.[22] Excited quinone radical anions have been implicated as the products of highly exoergic electron-transfer reactions.[23] Nevertheless, the excited states of organic radical anions have not been studied widely in condensed media.

Aromatic diimides have been used as electron acceptors in many fundamental studies of photoinduced electron-transfer including models for photosynthesis,[24−28] solar energy conversion,[29] molecular electronics,[30] electrochromic devices,[31,32] and photorefractive materials.[33,34] These molecules have been widely used in electron-transfer studies because they undergo reversible one-electron reduction at modest potentials to form stable radical anions. In addition, the radical anions of most aromatic diimides are good chromophores with intense and characteristic visible and near-infrared (NIR) absorption bands, which aid in their unambiguous identification. The diimides studied here also possess stable doubly reduced dianions with properties that differ from either their neutral or radical anion precursors. The electrochemical and photophysical properties of some aromatic mono-, di-, and polyimides have been previously reported;[35−38] however, very little is known about the excited states of the radical anions of these important electron acceptors. We have therefore undertaken a systematic study of the excited doublet states of the radical anions within a series of aromatic imides and diimides.

Results and Discussion

Electrochemistry. The cyclic voltammograms for all of the compounds showed two quasi-reversible (ΔE_p(anodic−cathodic) 59−88 mV at 50 mV·s^{-1}), well-separated one-electron reduction waves. Table 1 lists the measured half-wave reduction potentials for radical anion ($E^{-}_{1/2}$) and dianion ($E^{2-}_{1/2}$) formation. The reduction potentials for molecules **1**−**6** (Chart 1) are all in agreement with previously reported values of the same or very similar compounds.[31,35−37,39] As previously noted, within the imide and diimide series the first and second reduction potentials become more positive as the core aromatic ring system

† E-mail: wasielew@chem.nwu.edu.

10.1021/jp000706f CCC: $19.00
Published on Web 06/24/2000

TABLE 1: Redox Potentials (V vs SCE)

compd	$E^{-}_{1/2}$	$E^{2-}_{1/2}$	$E^{2-}_{1/2} - E^{-}_{1/2}$
1	−1.40[36]	−2.30[36]	0.90
2[a]	−1.365		
3[a]	−0.96	−1.55	0.59
4a,**b**[b]	−0.71	−1.37	0.66
5a,**b**[b]	−0.48	−0.99	0.51
6[b]	−0.43	−0.70	0.27

[a] Butyronitrile + 0.1 M Bu_4NPF_6. [b] DMF + 0.1 M Bu_4NPF_6.

CHART 1

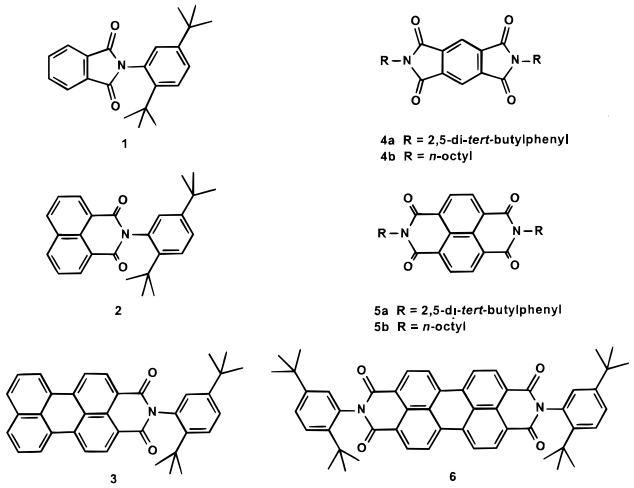

becomes larger.[35] In addition, the reduction potentials of the diimides are all more positive than those of the monoimides. Furthermore, within each series, the difference between the first and second reduction potential ($\Delta E^0 = E^{2-}_{1/2} - E^{-}_{1/2}$) becomes smaller with increased core size.[31] These two observations indicate that the more extended π systems have larger electron affinities and diminished Coulombic repulsion between the first and second electrons added to the ring system during reduction.

Radical Anion and Dianion Spectra. Ground-state absorption spectra of the radical anions of **1**−**3** are shown in Figure 1, while absorption spectra of the neutral (**N**), radical anion ($\mathbf{R}^{\bullet-}$), and dianion ($\mathbf{R}^{2-}$) states of **4**−**6** are shown in Figure 2. Wavelengths and extinction coefficients of the major absorption bands for the various oxidation states are listed in Table 2. Bulk electrolysis from $\mathbf{N} \rightarrow \mathbf{R}^{\bullet-} \rightarrow \mathbf{R}^{2-} \rightarrow \mathbf{N}$ for diimides **4**−**6** is almost completely reversible with greater than 90% recovery of **N** after more than 30 min at the most negative potentials. Most of the loss is probably due to reactions with residual oxygen within the optically transparent, thin layer electrochemical (OTTLE) cell, although some loss, especially during potential excursions to the dianion states, may be due to photodegradation (vide infra). Bulk electrochemical reduction of monoimides **1**−**3** to $\mathbf{R}^{\bullet-}$ is found to be somewhat less reversible than is observed for the diimides. Again, the partial irreversibility is probably due to scavenging by oxygen or photodegradation and the fact that the first reduction potential for the monoimides is consistently more negative than even the second reduction potential of the diimides. Extinction coefficients for the $\mathbf{R}^{\bullet-}$ absorption bands are calculated by comparing peak intensity ratios between the growing $\mathbf{R}^{\bullet-}$ and decaying **N** absorption bands during the first electroreduction step. Likewise, extinction coefficients for the $\mathbf{R}^{2-}$ absorption bands are calculated by comparing peak intensity ratios between the growing $\mathbf{R}^{2-}$ and decaying $\mathbf{R}^{\bullet-}$ bands during the second electroreduction step. The 0.27−0.66 V separation between $E^{-}_{1/2}$ and $E^{2-}_{1/2}$ permitted bulk reduction to be carried out in two discrete steps. This was confirmed by the detection of at least one isosbestic point during the formation of $\mathbf{R}^{\bullet-}$ in all of the compounds except **1** and **4**, which are the only compounds in which there is no spectral overlap between the **N** and $\mathbf{R}^{\bullet-}$ oxidation states. During the second reduction step, new isosbestic points were detected for **4**−**6** as $\mathbf{R}^{2-}$ was formed.

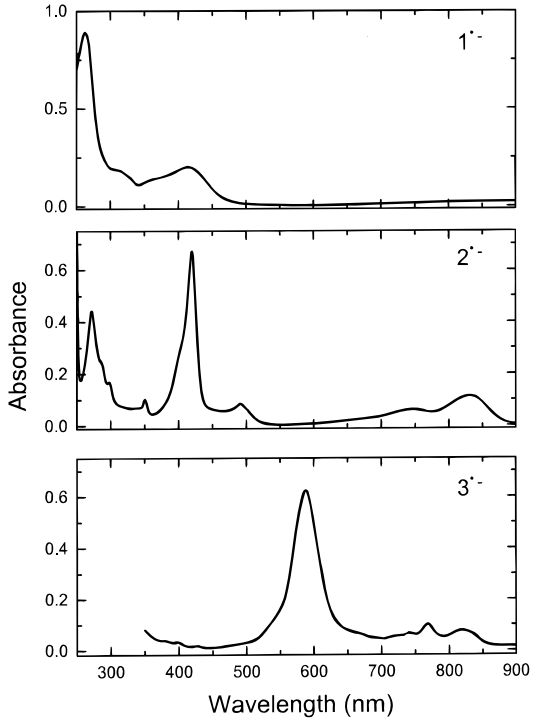

Figure 1. Ground-state absorption spectra of electrochemically generated radical anions of **1**−**3** in DMF + 0.1 M Bu_4NPF_6.

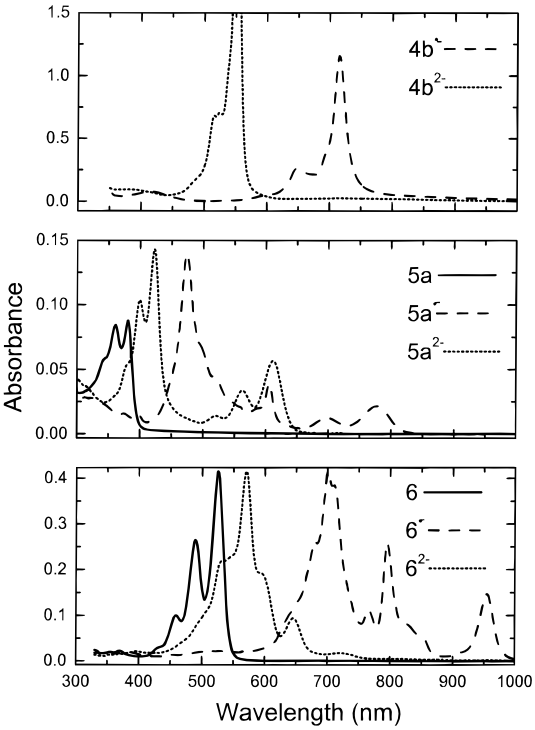

Figure 2. Ground-state absorption spectra of neutral, radical anion, and dianion forms of **4b**, **5a**, and **6** in DMF + 0.1 M Bu_4NPF_6.

Upon formation of $\mathbf{R}^{\bullet-}$, the absorption spectra of all of the compounds show new bands throughout the visible and NIR.

TABLE 2: Photophysical Properties

compd	**N**: λ (nm) (ϵ (M^{-1} cm^{-1}))	$\mathbf{R}^{\bullet-}$: λ (nm) (ϵ (M^{-1} cm^{-1}))	$\mathbf{R}^{2-}$: λ (nm) (ϵ (M^{-1} cm^{-1}))	^{1*}**N**: τ (ps)	$^{2*}\mathbf{R}^{\bullet-}$: τ (ps)
1		260 (15 600)		185[44]	
		419 (3470)[36]			
2	335 (12 500)[38]	272 (15 500)		<50[42]	
	350 (10 647)	420 (23 500)			
		491 (3000)			
		746 (2200)			
		832 (4000)			
3	489 (35 300)[55]	588 (68 000)		3500 ± 100	533 ± 57
	512 (33 590)	768 (11 000)			
		818 (8500)			
4a		406 (2700)			6 ± 2
		652 (9800)			
		718 (41 700)[36]			
4b		418 (2700)	516 (23 300)		9 ± 2
		649 (9400)	525 (24 200)		
		715 (41 700)[36]	552 (14 4000)		
5a	361 (15 100)	474 (26 000)	400 (19 500)		141 ± 7
	381 (16 400)	605 (7200)	423 (26 700)		
		698 (2400)	520 (2600)		
		777 (4100)	563 (6300)		
			612 (10 600)		
5b	382 (14 500)[24]	474 (23 000)	397 (18 400)	<20[43]	260 ± 19
		605 (6400)	421 (28 400)		
		683 (2100)	510 (2300)		
		755 (3600)	550 (6600)		
			597 (11 500)		
6	458 (19 300)	680 (50 600)	532 (42 400)	3800 ± 100	145 ± 15
	490 (51 000)	700 (79 800)	570 (80 000)		
	526 (80 000)[39]	712 (74 200)	597 (36 700)		
		766 (21 600)	646 (18 100)		
		795 (49 600)	720 (3400)		
		955 (28 200)			

In general, all of the $\mathbf{R}^{\bullet-}$ spectra share a number of similarities: at least one long wavelength (>700 nm) absorption, which has been assigned to the $D_0 \rightarrow D_1$, transition of the radical anion,[35,36] intense transitions with extinction coefficients equal to or greater than those of the neutral compound, and complex vibronic structure on the absorption bands. Similar generalizations can be made with regard to the dianion spectra of **4**−**6** with the notable exception that no NIR absorption bands are present at wavelengths < 1100 nm. The singlet−singlet transitions in the dianions occur at higher energies than the doublet−doublet transitions in the radical anions.

To aid in interpreting the radical anion and dianion spectra, especially with regard to identifying the lowest energy transitions, molecular orbital calculations were performed. We calculated energy minimized ground-state structures of the radical anions and dianions of the *N*,*N*′-dimethyl-substituted analogues of **1**−**6** using semiempirical unrestricted and restricted Hartree−Fock PM3 methods, respectively. The energy-minimized structures were then subjected to a ZINDO/S calculation with CI to determine the electronic transition energies. These data are given in Table 3. The radical anions all possess low-energy transitions that correspond to $D_0 \rightarrow D_1$. Moreover, both the number and intensities of the predicted allowed transitions are in reasonable agreement with the observed radical anion spectra. The predicted transition energies for the diimides agree reasonably well with experiment, while those for the monoimides agree less so.

Within the series of monoimides, the MO calculations predict $D_0 \rightarrow D_1$ transitions with modest intensities in the NIR. Low-energy absorption bands are observed for $\mathbf{2}^{\bullet-}$ and $\mathbf{3}^{\bullet-}$ at 832 and 818 nm, respectively. These bands correspond to the calculated transitions at 957 and 836 nm for the *N*-methyl derivatives of $\mathbf{2}^{\bullet-}$ and $\mathbf{3}^{\bullet-}$, respectively, and are thus assigned to this transition. The lowest energy transition predicted for $\mathbf{1}^{\bullet-}$ at 1037 nm is weak and is not observed experimentally. However, the spectrum of $\mathbf{1}^{\bullet-}$ shown in Figure 1 displays a slight increase in the baseline at NIR wavelengths.

TABLE 3: Calculated Electronic Transitions for Radical Anions and Dianions

	λ_{max} (nm) (osc strength)	
compd	radical anion	dianion
N-methylphthalimide	257 (0.135)	370 (0.356)
	559 (0.133)	600 (0)
	1037 (0.024)	734 (0.067)
N-methyl-1,8-naphthalimide	435 (0.105)	401 (0.564)
	438 (0)	515 (0.409)
	656 (0.111)	704 (0.038)
	907 (0.018)	
	957 (0.073)	
N-methylperylene-3,4-dicarboximide	553 (0.896)	470 (0.208)
	601 (0.004)	496 (1.177)
	747 (0.085)	497 (0.123)
	836 (0.007)	586 (0.122)
N,*N*′-dimethyl-pyromellitimide	396 (0.142)	514 (0.960)
	785 (0.207)	733 (0)
	916 (0)	
N,*N*′-dimethylnaphthalene-1,8:4,5-tetracarboxydiimide	474 (0.540)	389 (0.998)
	575 (0.045)	484 (0)
	628 (0)	545 (0.468)
	839 (0.097)	
N,*N*′-dimethylperylene-3,4:9,10-tetracarboxydiimide	615 (1.090)	429 (0.116)
	724 (0.105)	436 (0)
	851 (0.014)	492 (1.510)
		526 (0.370)

If one compares the energy differences between the predicted electronic transitions for the diimides with the corresponding energy differences in the observed spectra, the agreement is good. This gives us confidence to assign the observed 777 and 955 nm bands in $\mathbf{5a}^{\bullet-}$ and $\mathbf{6}^{\bullet-}$ respectively to their $D_0 \rightarrow D_1$ transitions. The calculations predict that the $D_0 \rightarrow D_1$ transition in $\mathbf{4}^{\bullet-}$ should be very weak at best, so that the intense band

observed at 715 nm is assigned to the allowed $D_0 \rightarrow D_2$ transition.

Typically, for rigid aromatic molecules the absorption spectrum of the π^* excited state of the neutral molecule (^{1*}**N**) strongly resembles that of the ground state of its radical anion (**R**$^{\bullet-}$). For example, ^{1*}**3** and **3**$^{\bullet-}$ both have an absorption band around 590 nm, whereas ^{1*}**6** and **6**$^{\bullet-}$ both have intense absorption bands around 700 nm. This similarity between the ^{1*}**N** and **R**$^{\bullet-}$ spectra can be attributed to the fact that both the $S_1 \rightarrow S_n$ and $D_0 \rightarrow D_n$ transitions involve the LUMO of **N**. In the case of ^{1*}**N**, the LUMO of **N** is populated by the initial photoexcitation of an electron from the HOMO of **N**. For **R**$^{\bullet-}$, the LUMO of **N** is populated by the one-electron electrochemical reduction of **N** forming the doublet ground state, D_0, of **R**$^{\bullet-}$. While the optical transitions observed for ^{1*}**N** are $S_1 \rightarrow S_n$ and the corresponding transitions for **R**$^{\bullet-}$ are $D_0 \rightarrow D_n$, both sets of transitions occur at similar energies. This is a consequence of the fact that the energy of the LUMO of **N** is not changed greatly if it is occupied by either one or two electrons. Excitation of an electron from the LUMO of **N** to higher-lying π orbitals of similar energy occurs as well. The rigidity of the molecules inhibits configurational mixing to some degree leading to spectra that can be analyzed by a zero-order consideration of the lowest populated π orbitals.

Table 3 also gives the calculated singlet−singlet electronic transitions for the dianions of **1**-**6**. The data for *N*-methyl **1**$^{2-}$−**3**$^{2-}$ are provided for completeness, but will not be discussed because the corresponding spectroelectrochemical data for **1**$^{2-}$−**3**$^{2-}$ could not be obtained due to the difficulty in producing the dianions by that method. The calculated singlet−singlet transitions for *N*,*N*′-dimethyl **4**$^{2-}$−**6**$^{2-}$ are in excellent agreement with the corresponding experimental data for **4**$^{2-}$−**6**$^{2-}$. For example, the intense transitions observed at 421 and 597 nm for **5a**$^{2-}$ are calculated to occur at 389 and 545 nm, respectively.

Radical Anion Excited-State Spectra. Transient absorption spectroscopy using 150 fs laser pulses was used to measure the transient difference spectra and lifetimes of the radical anion excited states (^{2*}**R**$^{\bullet-}$) of compounds **1**−**6**. The radical anion excited states were formed by exciting one of the intense $D_0 \rightarrow D_n$ transitions of **R**$^{\bullet-}$. Laser excitation of **R**$^{\bullet-}$ was usually not directed into the lowest energy, $D_0 \rightarrow D_1$, transition since the higher energy visible transitions often have much larger extinction coefficients than the NIR transitions and occur within the convenient tuning range of the pump laser. Excited-state transient absorption difference spectra of **3**$^{\bullet-}$−**6**$^{\bullet-}$ are shown in Figure 3. Radical anions **3**$^{\bullet-}$−**6**$^{\bullet-}$ were excited at 590, 715, 605, and 700 nm, respectively. While scattered laser light distorts the spectra to varying degrees at the pump wavelength, the transient spectra at the other wavelengths consist primarily of ground-state bleaching bands with very little positive ΔA. For example, the transient absorption spectrum of ^{2*}**5a**$^{\bullet-}$ shown in Figure 3 exhibits a strong bleach of the 474 nm band of **5a**$^{\bullet-}$ at 12 ps following excitation but only slight positive ΔA changes near 650 nm. However, in addition to their ground-state bleaching features, ^{2*}**3**$^{\bullet-}$ and ^{2*}**6**$^{\bullet-}$ also show strong positive ΔA features below about 500 nm. The transient spectrum of each of the excited radical anions shows no evidence for formation of solvated electrons generated by means of photoionization of the radical anions.

Radical Anion Excited-State Lifetimes. Although there have been relatively few direct measurements of the excited-state lifetimes of radical anions, it has been proposed that they will have shorter lifetimes than the neutral parent due to the relatively small energy gap between the D_0 and D_1 states, giving rise to rapid and efficient nonradiative decay to the ground state.[14,40] Moreover, if the transitions are $\pi-\pi^*$ in nature, their lifetimes may not be limited by symmetry considerations. The excited-state lifetimes of ^{2*}**R**$^{\bullet-}$ were determined by monitoring both the recovery of the **R**$^{\bullet-}$ ground state as well as the decay of the transient spectra due to ^{2*}**R**$^{\bullet-}$. The lifetimes measured for the excited states of the radical anions of **3**−**6** are listed in Table 2.

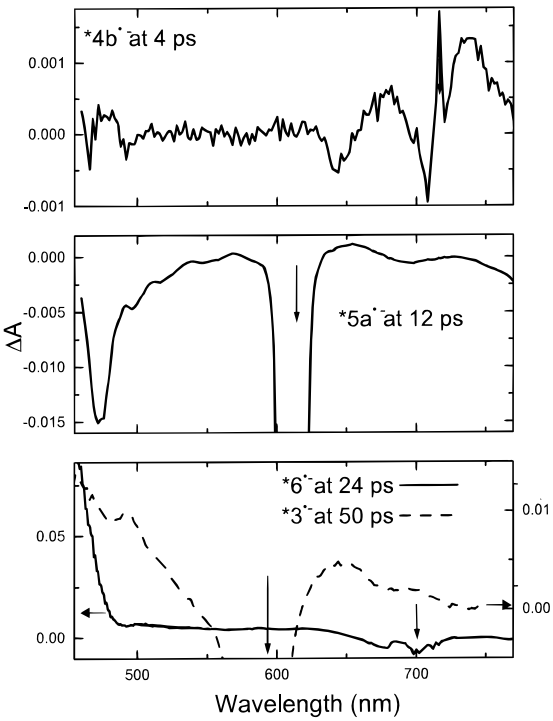

Figure 3. Transient absorption spectra of radical anions of **4b**, **5a**, **6**, and **3**. Pump wavelengths are indicated by the vertical arrows. The spectra are distorted at the pump wavelengths due to scattered laser light. Times are given for the delay of the probe beam relative to the excitation beam.

The subnanosecond excited-state lifetimes of the diimide radical anions may contribute to their exceptional photostability, since radical anion excited states are generally extraordinarily strong reducing agents.[1,4] For example, the oxidation potential for the excited doublet state ^{2*}**4**$^{\bullet-}$ can be estimated[41] from the difference between the oxidation potential of the radical anion, −0.71 V vs SCE, and the calculated energy of the $D_0 \rightarrow D_1$ transition, 1.4 eV, to give an oxidation potential of −2.1 V vs SCE. Since the lifetime of ^{2*}**4a**$^{\bullet-}$ is only 6 ps, its excited-state energy may dissipate before any intermolecular redox chemistry can occur. For **1** and **2**, the two most difficult to reduce compounds, the excited-state lifetimes of ^{2*}**1**$^{\bullet-}$ and ^{2*}**2**$^{\bullet-}$ could not be determined due to rapid decomposition of the excited radical anions. Even at pump energies as low as 100 nJ/pulse, the sample volume bleached in a matter of seconds. The design of the spectroelectrochemical cell used in these experiments is such that the only mass transport mechanism available to replenish the bleached sample volume is diffusion. Calculated as above, the oxidation potentials of ^{2*}**1**$^{\bullet-}$ and ^{2*}**2**$^{\bullet-}$ are about −2.7 V vs SCE, a potential that may be sufficiently negative to rapidly reduce the solvent and/or the electrolyte.

For compounds **3**−**6**, which were initially excited into higher-lying D_n states, the **R**$^{\bullet-}$ ground-state recovery time is the same as the ^{2*}**R**$^{\bullet-}$ decay time indicating that rapid relaxation to the D_1 state within the doublet manifold of ^{2*}**R**$^{\bullet-}$ occurs. In all cases, ^{2*}**R**$^{\bullet-}$ is formed with an instrument limited rise time and decays with a single-exponential time constant. For example, excitation

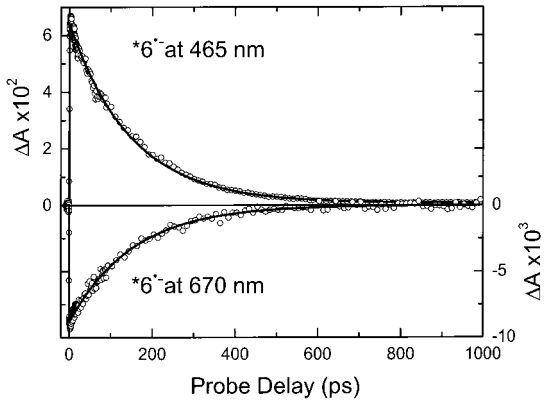

Figure 4. Excited-state transient absorption decay kinetics of radical anion of **6** in DMF + 0.1 M Bu_4NPF_6. Laser excitation at 715 nm was used in both cases.

of $\mathbf{6}^{\bullet-}$ at its 700 nm absorption band, which is three times more intense than its lowest energy $D_0 \rightarrow D_1$ transition at 955 nm, yields the same 145 ps time constant independent of whether its bleach recovery at 670 nm or its small positive ΔA at 465 nm is monitored, Figure 4. These results show that internal conversion from higher-lying D_n states occurs rapidly in these molecules without intersystem crossing to a long-lived quartet state.[7]

For the two perylene-based molecules, **3** and **6**, the excited state lifetimes of the radical anions are substantially shorter than the excited-state lifetimes of the neutral molecules as expected from the lower energy transitions involved. Contrasting with this behavior are the significantly longer lifetimes of the radical anion excited states of the naphthalene-based molecules, $^{2*}\mathbf{5a}^{\bullet-}$ and $^{2*}\mathbf{5b}^{\bullet-}$, 141 and 260 ps, respectively, compared to the <20 ps lifetime of neutral $^{1*}\mathbf{5b}$. The <50 ps lifetime of both $^{1*}\mathbf{2}$ and $^{1*}\mathbf{5b}$ has been attributed to both efficient singlet → triplet intersystem crossing and to very fast internal conversion.[42−44] The increase in the excited-state lifetimes of radical anions $^{2*}\mathbf{5a}^{\bullet-}$ and $^{2*}\mathbf{5b}^{\bullet-}$ over their neutral counterparts implies that the rates of competitive decay processes, such as intersystem crossing and internal conversion, are slower for the $D_1 \rightarrow D_0$ transition than for the corresponding $S_1 \rightarrow S_0$ transition.

The effect of the imide substituent on the radical anion excited-state lifetime was investigated by comparing *N*,*N*′-bis-(2,5-di-*tert*-butylphenyl) and *N*,*N*′-di-*n*-octyl substituents on pyromellitimide and naphthalene-1,8:4,5-tetracarboxydiimide. Perylene-3,4:9,10-tetracarboxydiimide was not included in the comparison due to the insolubility of its *N*,*N*′-di-*n*-octyl derivative. The variation in imide substituent had no effect on the absorption spectra of the neutral molecules nor on their redox properties. Differences were, however, apparent between the spectra of the radical anions and dianions as well as in the lifetimes of the radical anion excited states. A comparison between the ground-state radical anion spectra of $\mathbf{5a}^{\bullet-}$ and $\mathbf{5b}^{\bullet-}$ or between the dianion spectra of $\mathbf{5a}^{2-}$ and $\mathbf{5b}^{2-}$ reveals that the lower energy absorption bands are red shifted for the *N*,*N*′-diaryl-substituted compound relative to the *N*,*N*′-dialkyl-substituted compound. The $D_0 \rightarrow D_1$ radical anion absorption band occurs at 380 cm^{-1} lower energy in $\mathbf{5a}^{\bullet-}$ than in $\mathbf{5b}^{\bullet-}$, while the $S_0 \rightarrow S_1$ dianion absorption band occurs at 400 cm^{-1} lower energy in $\mathbf{5a}^{2-}$ than in $\mathbf{5b}^{2-}$. The lower energy transitions in the *N*,*N*′-diaryl-substituted reduced diimides suggest that even though the *N*-phenyl rings are tilted out of the plane of the aromatic diimide as a consequence of steric hindrance between the 2-*tert*-butyl group and the imide carbonyl groups, there may be enough π overlap between the *N*,*N*′-diaryl substituents and the aromatic diimide to partially delocalize electron density onto the *N*,*N*′-diaryl substituents. These results are also consistent with *N*-substitution studies of 1,8-naphthalimides in which it was shown that the fluorescence lifetime was longer and the fluorescence quantum yield was larger for the *N*-methyl- versus *N*-phenyl-substituted imide.[42,44] The excited-state radical anion lifetimes of $^{2*}\mathbf{4a}^{\bullet-}$ vs $^{2*}\mathbf{4b}^{\bullet-}$ and $^{2*}\mathbf{5a}^{\bullet-}$ vs $^{2*}\mathbf{5b}^{\bullet-}$ also show a substituent effect in that the excited-state lifetimes of the *N*,*N*′-diaryl substituted radical anions are shorter than those of the corresponding *N*,*N*′-dioctyl compounds, 6 ps vs 9 ps for $^{2*}\mathbf{4a}^{\bullet-}$ and $^{2*}\mathbf{4b}^{\bullet-}$, respectively, and 140 ps vs 260 ps for $^{2*}\mathbf{5a}^{\bullet-}$ and $^{2*}\mathbf{5b}^{\bullet-}$, respectively. The red-shifted radical anion spectra suggest that the D_0-D_1 energy gap is smaller in the *N*,*N*′-diaryl-substituted diimides. As a consequence, the energy gap law[45] predicts shorter lifetimes for the *N*,*N*′-diaryl-substituted diimides.

An examination of the data in Table 2 shows that the lifetimes of the diimide radical ions are ordered in the following series: $\mathbf{4a}^{\bullet-} < \mathbf{5a}^{\bullet-} \cong \mathbf{6}^{\bullet-}$. This is also the order in which **4**−**6** become easier to reduce. As the one-electron reduction potentials for these molecules become more negative, the energies of D_0 increase. This may result in a decrease in the D_0-D_1 gap, which should decrease the lifetime of $^{2*}\mathbf{R}^{\bullet-}$. However, this does not take into account the effects of structure on the energy of the D_1 state. The measured D_0-D_1 energy gaps for $\mathbf{5a}^{\bullet-}$ and $\mathbf{6}^{\bullet-}$ are 12 870 and 10 470 cm^{-1}, respectively. Thus, the difference between the observed D_0-D_1 gaps for $\mathbf{5a}^{\bullet-}$ and $\mathbf{6}^{\bullet-}$ primarily reflects the difference in their D_1 energy levels because both **5a** and **6** are reduced at approximately the same redox potential. Despite the 2400 cm^{-1} difference in the observed D_0-D_1 energy gap between **5a** and **6**, they possess similar radical anion excited-state lifetimes. If predictions of the radical anion excited-state lifetimes based on the energy gap law are valid for the **4**−**6**, the experimental results suggest that the D_0-D_1 energy gap for $\mathbf{4}^{\bullet-}$ should be substantially lower in energy than the 10 920 cm^{-1} value calculated by ZINDO/S. In fact, density functional calculations using the B3LYP method with a 6-31G* basis set predict that the D_0-D_1 energy gap for pyromellitic dianhydride is about 8100 cm^{-1}.[46] These same calculations accurately predict the experimentally observed $D_0 \rightarrow D_2$ transition in $\mathbf{4}^{\bullet-}$ near 715 nm. Thus, it is likely that the observed ordering of radical anion excited-state lifetimes observed in **4**−**6** is a function of the D_0-D_1 energy gap.

Conclusions

The results presented here provide design criteria for electron donor−acceptor systems that use the powerful reducing potential of the radical anion excited states of aromatic imides and diimides and which take advantage of the highly electrochromic nature of the multiple reduced states of these molecules. These constraints mainly involve designing donor−acceptor molecules in which the electronic couplings and free energies of reaction are sufficiently optimized to ensure ultrafast electron transfer from the short-lived radical anion excited states of the aromatic diimides to attached acceptors. This selectivity has already been used in diimide-containing linear and branched donor−acceptor molecules that have demonstrated photonic switching behavior on the basis of electron transfer from radical anion excited states.[30,47]

Also, it has been suggested that photoexcited radical anions may be very useful in studying fundamental aspects of electron transfer.[17] The radical anions of the diimides in particular are well suited to this task because they are weakly basic relative to quinones and are thus less susceptible to complicating proton transfer reactions. In addition, they can be excited with visible

light and their highly energetic excited states allow access to electron-transfer reactions that occur in the Marcus inverted region. These highly energetic excited radical anions may also be useful as photoelectrochemical catalysts by acting as electron shuttles. The absorption spectra of the radical anions of the easiest to reduce diimides, **5** and **6**, cover much of the solar spectrum. Experiments are currently underway to study photoinduced charge shift reactions involving electrochemically reduced diimides.

Experimental Section

Reagents. *N*,*N*-Dimethylformamide (DMF, Mallinckrodt) and butyronitrile (Mallinckrodt) were purged with N_2 and stored over molecular sieves prior to use. Tetrabutylammonium hexafluorophosphate (Bu_4NPF_6) was synthesized by metathesis between tetrabutylammonium bromide (Aldrich) and potassium hexafluorophosphate (Aldrich) and recrystallized twice from methanol.[48]

N-(2,5-Di-*tert*-butylphenyl)-3,4-perylenedicarboximide,[49] **3**, *N*,*N*′-bis-(*n*-octyl)pyromellitimide,[50] **4b**, and *N*,*N*′-dioctyl-1,8:4,5-naphthalenetetracarboxydiimide,[24] **5b**, were synthesized by utilizing published procedures. *N*,*N*′-Bis(2,5-di-*tert*-butylphenyl)-3,4:9,10-perylenetetracarboxydiimide, **6**, was purchased from Aldrich. The syntheses of *N*-(2,5-di-*tert*-butylphenyl)phthalimide, **1**, *N*-(2,5-di-*tert*-butylphenyl)-1,8-naphthalimide, **2**, *N*,*N*′-bis(2,5-di-*tert*-butylphenyl)pyromellitimide, **4a**, and *N*,*N*′-bis-(2,5-di-*tert*-butylphenyl)-1,8:4,5-naphthalenetetracarboxydiimide, **5a**, are presented in the Supporting Information.

Electrochemistry. Cyclic voltammetry (CV) and bulk electrolysis were carried out using a computer-controlled potentiostat (Princeton Applied Research, model 273, M270 software package) and a standard three electrode arrangement. CV measurements used both platinum working and auxiliary electrodes and a saturated sodium calomel reference electrode (SSCE). All electrochemical measurements were carried out in N_2-purged DMF or butyronitrile with 0.1 M Bu_4NPF_6 as the supporting electrolyte. The scan rate for CV measurements was typically 50−100 mV/s. Ferrocene was used as an internal redox standard for all potentiometric measurements. Bulk electrolyses for anion and dianion ground-state spectra were carried out in an optically transparent thin layer electrochemical cell (OTTLE)[51,52] utilizing a 2 cm^2, 250 lines/in., gold minigrid working electrode. Bulk electrolysis for the transient experiments also utilized the OTTLE.

Spectroscopy. Ground-state absorption measurements of neutral and reduced species were recorded using a computer-controlled spectrophotometer (Shimadzu, model 1601). Absorption spectra of the electrochemically generated anions and dianions were recorded by passing the light beam from the spectrophotometer through the minigrid electrode, which had an optical density of about 0.3. A blank spectrum consisting of the OTTLE filled with solvent and supporting electrolyte was subtracted from each data set.

Transient absorption spectra and kinetics of the neutral and electrochemically generated radical anions were recorded using a previously described amplified titanium:sapphire laser system[24,53] pumping a tunable optical parametric amplifier (OPA).[54] Briefly, the output from a continuous wave, intracavity-doubled Nd:YVO_4 laser (Spectra Physics Millenia) pumped a self-modelocked titanium:sapphire oscillator operating at 840 nm. The 50 fs 840 nm output was temporally stretched, amplified with a regenerative titanium:sapphire amplifier pumped with the output from a frequency-doubled 1 kHz Nd:YLF (Quantronix, 527DP-S) and then temporally recompressed. The compressed output (150 fs) of the amplifier was split with about 5% used to make a stable white light continuum probe beam by focusing it into a 2 mm thick sapphire window. The remaining amplified light was doubled yielding 60−100 μJ, 420 nm pulses. The doubled light was used to pump a two stage OPA, which was tunable from 475 to 750 nm. Samples were typically excited using 0.5 μJ focused to ca. 200 μm.

MO Calculations. Molecular orbital calculations were carried out using the semiempirical Hartree−Fock technique with PM3 parametrization within the Hyperchem package (Waterloo, Ontario, Canada). The ground-state structures of the radical anions were calculated using an unrestricted basis set, whereas the dianions structures were calculated using a restricted basis set. The ground-state structures were then subjected to a ZINDO/S CI calculation using 163 configurations for the dianions and 162 configurations for the radical anions.

Acknowledgment. Work at ANL was supported by the Division of Chemical Sciences, Office of Basic Energy Sciences, Department of Energy, under Contract W-31-109-Eng-38. Work at Northwestern was supported by the National Science Foundation (Grant CHE-9732840).

Supporting Information Available: Text describing the synthesis and characterization of compounds **1**, **2**, **4a**, and **5a** . This material is available free of charge via the Internet at http://pubs.acs.org.

References and Notes

(1) Fox, M. A. *Chem. Rev.* **1979**, *79*, 253−73.
(2) Moutet, J. C.; Reverdy, G. *J. Chem. Soc., Chem. Commun.* **1982**, 654−5.
(3) Shukla, S. S.; Rusling, J. F. *J. Phys. Chem.* **1985**, *89*, 3353−8.
(4) Eriksen, J. *In-situ generated intermediates*; Fox, M. A., Chanon, M., Eds.; Elsevier: Amsterdam, 1988; Vol. Pt. A, pp 391−408.
(5) Shine, H. J.; Zhao, D. C. *J. Org. Chem.* **1990**, *55*, 4086−9.
(6) Legros, B.; Vandereecken, P.; Soumillion, J. P. *J. Phys. Chem.* **1991**, *95*, 5, 4752−61.
(7) Eggins, B. R.; Robertson, P. K. J. *J. Chem. Soc., Faraday Trans.* **1994**, *90*, 2249−56.
(8) Majima, T.; Fukui, M.; Ishida, A.; Takamuku, S. *J. Phys. Chem.* **1996**, *100*, 8913−19.
(9) Tokumura, K.; Mizukami, N.; Udagawa, M.; Itoh, M. *J. Phys. Chem.* **1986**, *90*, 3873−3876.
(10) Scaiano, J. C.; Johnston, L. J.; McGimpsey, W. G.; Weir, D. *Acc. Chem. Res.* **1988**, *21*, 22−9.
(11) Tokumura, K.; Ozaki, T.; Udagawa, M.; Itoh, M. *J. Phys. Chem.* **1989**, *93*, 161−164.
(12) Samanta, A.; Bhattacharyya, K.; Das, P. K.; Kamat, P. V.; Weir, D.; Hug, G. L. *J. Phys. Chem.* **1989**, *93*, 3651−3656.
(13) Filatov, I. V.; Chirvonyi, V. S.; Sinyakov, G. N. *Opt. Spektrosk.* **1994**, *77*, 386−8.
(14) Breslin, D. T.; Fox, M. A. *J. Phys. Chem.* **1994**, *98*, 408−11.
(15) Filatov, I. V.; Chirvony, V. S.; Sinyakov, G. N. *Proc. SPIE-Int. Soc. Opt. Eng.* **1995**, *2370*, 95−8.
(16) Ishida, A.; Fukui, M.; Ogawa, H.; Tojo, S.; Majima, T.; Takamuku, S. *J. Phys. Chem.* **1995**, *99*, 10808−14.
(17) Cook, A. R.; Curtiss, L. A.; Miller, J. R. *J. Am. Chem. Soc.* **1997**, *119*, 5729−5734.
(18) Fujisawa, J.; Ishii, K.; Ohba, Y.; Yamauchi, S.; Fuhs, M.; Mobius, K. *J. Phys. Chem. A* **1999**, *103*, 213−216.
(19) Ishii, K.; Hirose, Y.; Kobayashi, N. *J. Phys. Chem. A* **1999**, *103*, 1986−1990.
(20) Brugman, C. J. M.; Rettschnick, R. P. H.; Hoytink, G. J. *Chem. Phys. Lett.* **1971**, *8*, 574−578.
(21) Daub, J.; Beck, M.; Knorr, A.; Spreitzer, H. *Pure Appl. Chem.* **1996**, *68*, 1399−1404.
(22) Wasielewski, M. R. *Chem. Rev.* **1992**, *92*, 435−61.
(23) Closs, G. L.; Calcaterra, L. T.; Green, N. J.; Penfield, K. W.; Miller, J. R. *J. Phys. Chem.* **1986**, *90*, 3673−3683.
(24) Greenfield, S. R.; Svec, W. A.; Gosztola, D.; Wasielewski, M. R. *J. Am. Chem. Soc.* **1996**, *118*, 6767−6777.
(25) Wiederrecht, G. P.; Niemczyk, M. P.; Svec, W. A.; Wasielewski, M. R. *J. Am. Chem. Soc.* **1996**, *118*, 81−8.
(26) Osuka, A.; Mataga, N.; Okada, T. *Pure Appl. Chem.* **1997**, *69*, 797−802.

(27) Osuka, A.; Marumo, S.; Okada, T.; Taniguchi, S.; Mataga, N.; Ohno, T.; Nozaki, K.; Yamazaki, I.; Nishimura, Y. *J. Photosci.* **1997**, *4*, 113−119.
(28) Levanon, H.; Galili, T.; Regev, A.; Wiederrecht, G. P.; Svec, W. A.; Wasielewski, M. R. *J. Am. Chem. Soc.* **1998**, *120*, 6366−6373.
(29) Angadi, M. A.; Gosztola, D.; Wasielewski, M. R. *J. Appl. Phys.* **1998**, *83*, 6187−6189.
(30) Debreczeny, M. P.; Svec, W. A.; Marsh, E. M.; Wasielewski, M. R. *J. Am. Chem. Soc.* **1996**, *118*, 8174−8175.
(31) Lee, S. K.; Zu, Y.; Herrmann, A.; Geerts, Y.; Mullen, K.; Bard, A. J. *J. Am. Chem. Soc.* **1999**, *121*, 3513−3520.
(32) Angadi, M. A.; Gosztola, D.; Wasielewski, M. R. *Mater. Sci. Eng., B* **1999**, *B63*, 191−194.
(33) Wiederrecht, G. P.; Wasielewski, M. R. *J. Am. Chem. Soc.* **1998**, *120*, 3231−3236.
(34) Wiederrecht, G. P.; Yoon, B. A.; Wasielewski, M. R. *Science (Washington, D.C.)* **1995**, *270*, 1794−7.
(35) Viehbeck, A.; Goldberg, M. J.; Kovac, C. A. *J. Electrochem. Soc.* **1990**, *137*, 1460−6.
(36) Rak, S. F.; Jozefiak, T. H.; Miller, L. L. *J. Org. Chem.* **1990**, *55*, 4794−801.
(37) Mazur, S.; Lugg, P. S.; Yarnitzky, C. *J. Electrochem. Soc.* **1987**, *134*, 346−53.
(38) Wintgens, V.; Valat, P.; Kossanyi, J.; Demeter, A.; Biczok, L.; Berces, T. *New J. Chem.* **1996**, *20*, 1149−1158.
(39) Ford, W. E.; Hiratsuka, H.; Kamat, P. V. *J. Phys. Chem.* **1989**, *93*, 6692−6.
(40) Gumy, J.-C.; Vauthey, E. *J. Phys. Chem. A* **1997**, *101*, 8575−8580.
(41) Julliard, M.; Chanon, M. *Chem. Rev.* **1983**, *83*, 425−506.
(42) Demeter, A.; Berces, T.; Biczok, L.; Wintgens, V.; Valat, P.; Kossanyi, J. *J. Phys. Chem.* **1996**, *100*, 2001−11.
(43) Green, S.; Fox, M. A. *J. Phys. Chem.* **1995**, *99*, 14752−7.
(44) Wintgens, V.; Valat, P.; Kossanyi, J.; Biczok, L.; Demeter, A.; Berces, T. *J. Chem. Soc., Faraday Trans.* **1994**, *90*, 411−21.
(45) Englman, R.; Jortner, J. *Mol. Phys.* **1970**, *18*, 145.
(46) Andruniow, T.; Pawlikowski, M.; Zgierski, M. Z. *J. Phys. Chem. A* **2000**, *104*, 845−851.
(47) Lukas, A. S.; Miller, S. E.; Wasielewski, M. R. *J. Phys. Chem. B* **2000**, *104*, 931−940.
(48) Fry, A. J. *Solvents and Supporting Electrolytes*, 2nd ed.; Kissinger, P. T., Heineman, W. R., Eds.; Marcel Dekker: New York, 1996; p 986.
(49) Langhals, H.; Grundner, S. *Chem. Ber.* **1986**, *119*, 2373−6.
(50) Debreczeny, M. P.; Svec, W. A.; Wasielewski, M. R. *New J. Chem.* **1996**, *20*, 815−828.
(51) Murray, R. W.; Heineman, W. R.; O'Dom, G. W. *Anal. Chem.* **1967**, *39*, 1666−8.
(52) DeAngelis, T. P.; Heineman, W. R. *J. Chem. Educ.* **1976**, *53*, 594−7.
(53) Gosztola, D.; Yamada, H.; Wasielewski, M. R. *J. Am. Chem. Soc.* **1995**, *117*, 2041−8.
(54) Greenfield, S. R.; Wasielewski, M. R. *Opt. Lett.* **1995**, *20*, 1394−6.
(55) Feiler, L.; Langhals, H.; Polborn, K. *Liebigs Ann.* **1995**, 1229−44.